JACS JOURNAL OF THE AMERICAN CHEMICAL SOCIETY

Communication

Cite This: J. Am. Chem. Soc. 2019, 141, 4230−4234

pubs.acs.org/JACS

Regioselective Hydrogenation of a 60-Carbon Nanographene Molecule toward a Circumbiphenyl Core

Xuelin Yao,[†] Xiao-Ye Wang,[†] Christopher Simpson,[†] Giuseppe M. Paternò,[‡] Michele Guizzardi,[§] Manfred Wagner,[†] Giulio Cerullo,[§] Francesco Scotognella,[‡,§] Mark D. Watson,[∥] Akimitsu Narita,*[,†,⊥] and Klaus Müllen*[,†,#]

[†]Max Planck Institute for Polymer Research, Ackermannweg 10, 55128 Mainz, Germany

[‡]Istituto Italiano di Tecnologia, Center for Nano Science and Technology, 20133 Milano, Italy

[§]IFN-CNR, Department of Physics, Politecnico di Milano, 20133 Milano, Italy

[∥]Department of Chemistry, University of Kentucky, Lexington, Kentucky 40506-0055, United States

[⊥]Organic and Carbon Nanomaterials Unit, Okinawa Institute of Science and Technology Graduate University, Okinawa 904-0495, Japan

[#]Institute of Physical Chemistry, Johannes Gutenberg University Mainz, Duesbergweg 10-14, 55128 Mainz, Germany

Supporting Information

ABSTRACT: Regioselective peripheral hydrogenation of a nanographene molecule with 60 contiguous sp^2 carbons provides unprecedented access to peralkylated circumbiphenyl (**1**). Conversion to the circumbiphenyl core structure was unambiguously validated by MALDI-TOF mass spectrometry, NMR, FT-IR, and Raman spectroscopy. UV−vis absorption spectra and DFT calculations demonstrated the significant change of the optoelectronic properties upon peripheral hydrogenation. Stimulated emission from **1**, observed via ultrafast transient absorption measurements, indicates potential as an optical gain material.

Large polycyclic aromatic hydrocarbons (PAHs),[1] i.e., with size >1 nm, can be regarded as nanographene molecules, and have attracted attention for their unique optical, electronic, and magnetic properties.[2] These properties are critically dependent on their aromatic core structure, motivating development of novel synthetic pathways to a variety of distinct aromatic frameworks.[3] Conventional synthetic strategies toward nanographene molecules are mostly based on π-expansion, mainly through planarization of tailor-made oligoarylene precursors, e.g., by oxidative cyclodehydrogenation,[4] photochemical cyclization,[5] and/or flash vacuum pyrolysis.[6] π-expansion of smaller PAH structures also provides access to larger PAHs, for example through Diels−Alder cycloaddition[7] or a sequence of arylation and cyclization at the periphery.[8]

Alternatively, it is possible to modify the aromatic structures of PAHs by "shrinking" the π-conjugated cores, for example through peripheral hydrogenation. We have previously reported that peripheral hydrogenation of hexa-*peri*-hexabenzocoronene (HBC) selectively leads to peralkylated coronenes.[9] More recently, Shionoya et al. described a catalytic reductive C−C bond cleavage of a corannulene derivative, leading to a benzo[*ghi*]fluoranthene structure.[10] On the other hand, "π-truncation" of aromatic structures has been applied to fullerene, with the formation of a hoop-shaped cyclic benzenoid compound by Nakamura et al. as one of the most elegant examples.[11] Nevertheless, compared with the π-expansion procedure, the "π-truncation" strategy is underdeveloped. We have been particularly interested in peripheral hydrogenation to produce new PAH or nanographene structures other than known skeletons such as coronene. However, hydrogenation of nanographene molecules larger than HBC has remained elusive.

Circumbiphenyl (**2**) is a PAH consisting of a biphenyl core encircled by an annulene ring (Figure 1). The parent **2** was accidentally obtained by E. Clar nearly half a century ago during his attempts to synthesize tetrabenzoperopyrene by

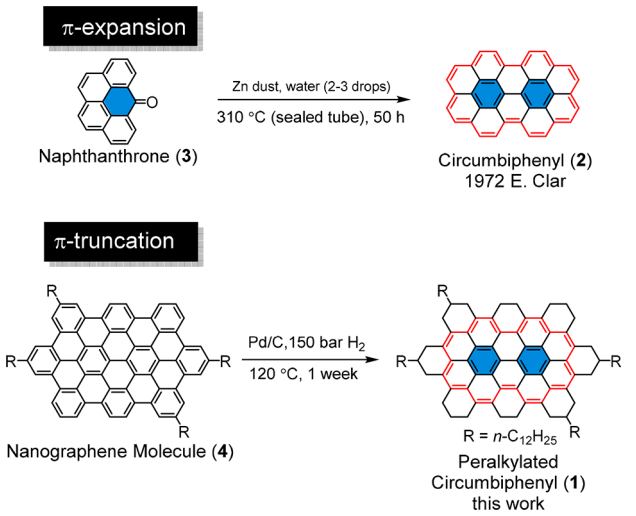

Figure 1. "π-Expansion" toward circumbiphenyl **2** by E. Clar and the postsynthetic "π-truncation" to peralkylated circumbiphenyl **1**.

Received: January 11, 2019
Published: February 22, 2019

DOI: 10.1021/jacs.9b00384
J. Am. Chem. Soc. 2019, 141, 4230−4234

reductive condensation of naphthanthrone (**3**).[12] However, this first reported synthetic approach yielded a complex mixture and required multistep separation processes to isolate **2**. In 2013, Nuckolls et al. reported a synthesis of a contorted octabenzocircumbiphenyl.[13] However, a straightforward and efficient synthesis of the pristine aromatic structure of circumbiphenyl has never been achieved.

Herein, we report an efficient synthesis of peralkylated circumbiphenyl **1** through "π-truncation", namely by regioselective hydrogenation of a nanographene molecule **4** with 60 sp^2 carbons (Figure 1). Standard spectroscopic characterization corroborates the successful formation of the circumbiphenyl core. UV−vis absorption spectroscopy combined with DFT calculations demonstrate the modulating effect of peripheral hydrogenation on electronic properties, while ultrafast spectroscopy highlights the presence of optical gain. This work offers possibilities not only for acquiring new or unobtainable aromatic structures but also for tuning (opto-)electronic properties of PAHs.

The synthesis of peralkylated circumbiphenyl **1** is outlined in Figure 1. The hydrogenation of nanographene molecule **4**, which was prepared following reported procedures,[14] was carried out with Pd/C in dry tetrahydrofuran (THF). The reaction mixture was pressurized to 150 bar H_2 and stirred at 120 °C in an autoclave for 1 week to complete the reaction. At a lower pressure of 120 bar and the same temperature of 120 °C, the hydrogenation needed 2 weeks for completion. These conditions are indeed much harsher than those used for the previous hydrogenation of HBC with six dodecyl chains (55−65 bar, 60 °C, 12 h).[9] After cooling, the catalyst was removed by passing through a short pad of silica gel with THF as eluent, and the crude product was obtained as yellowish brown powder in 30% yield.

High-resolution MALDI-TOF MS analyses of **4** and the hydrogenation product revealed exact mass of m/z = 1414.9216 and 1437.0945, respectively, in agreement with the formation of **1** ($C_{108}H_{140}$) possessing 22 more hydrogen atoms than **4** ($C_{108}H_{118}$) (Figure 2). The isotopic distribution observed for **1** perfectly matched the simulated pattern, validating the successful hydrogenation of **4**. Compound **1** was soluble even in *n*-hexane (0.65 mg/mL), in which **4** showed little solubility. Both the room-temperature and high-temperature ^{1}H NMR spectra of **1** revealed the disappearance of signals from protons attached to aromatic systems and

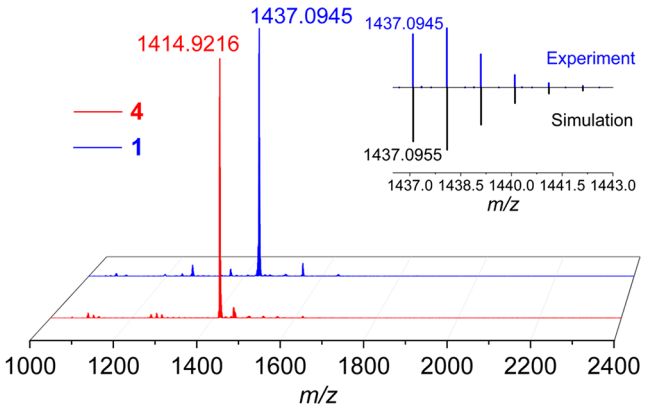

Figure 2. High-resolution MALDI-TOF MS spectrum of **1** and **4** (inset: the corresponding experimental and simulated isotopic distributions of **1**).

appearance of new signals in the aliphatic region, indicating the peripheral hydrogenation of **4**. 2D NMR analyses of **1** could distinguish different aliphatic proton signals originating from > CH−, $-CH_2-$ and $-CH_3$ (NMR spectra see Figures S1−S6 in the Supporting Information). However, accurate assignment of each proton signal of **1** was hampered by the existence of multiple diastereotopic peripheral protons and ^{1}H signal overlap. Compound **1** might consist of multiple stereoisomers, depending on the relative orientations of the four alkyl chains, which is under further investigation in our laboratory.

FT-IR spectroscopic analysis of **1** and **4** demonstrates the disappearance of aromatic C−H stretching bands at around 3073 cm^{-1},[15] as well as the fingerprint aromatic C−H bending bands between 730 and 860 cm^{-1}, corroborating peripheral hydrogenation (Figure 3, for full spectra, see Figure S7).

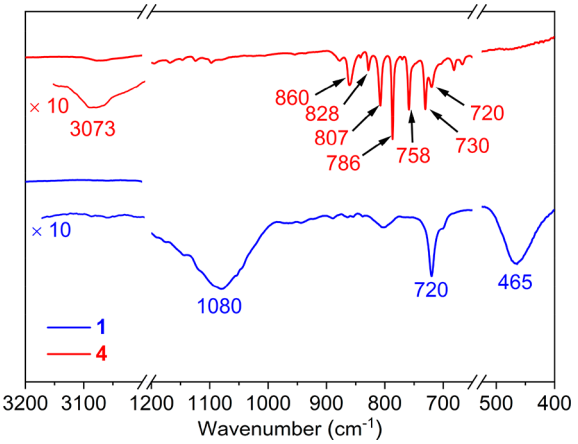

Figure 3. Representative FTIR spectra regions of **1** (blue line) and **4** (red line) measured on powder samples.

Additionally, appearance of bands at 1080 and 465 cm^{-1} from the saturated C−C stretching vibrations and out-of-plane bending, respectively, verifies the hydrogenated periphery of **1**.[16] In Raman spectra (Figure S8), the ratios between D and G bands, $I(D)/I(G)$ for **4** and **1** are 0.50 and 0.56, respectively, in accordance with the fact that $I(D)/I(G)$ varies inversely with the extension of the π-conjugation.[17]

In contrast to the broad optical spectra of **4**, which could be ascribed to the presence of aggregates,[18] those of **1** (THF solution, see Figure 4a) reveal well-resolved vibronic structures, indicating a significant improvement of solubility after peripheral hydrogenation, suppressing the aggregation.[19] The absorption maximum of **1** (λ_{max} = 381 nm) exhibits a significant blue-shift with respect to **4** (λ_{max} = 411 nm), indicating truncation of the π-skeleton. Notably, the absorption profile of peralkylated circumbiphenyl **1** perfectly matches that of the parent circumbiphenyl **2** (absorption maximum: 364 nm) reported by E. Clar,[12] with a red-shift of the absorption maximum by 17 nm. Peralkylated circumbiphenyl **1** displays a green fluorescence with the emission maximum at 512 nm. The fluorescence quantum yield Φ_F of **1** was measured as 12% using 9,10-diphenylanyhracene (in toluene under air, Φ_F: 70%) as reference.[20] Compound **4** exhibits a broad fluorescence peaking at 700 nm. The broad peak originates from aggregation, as revealed by concentration-dependent fluorescence studies, whereas the emission maximum of the monomer

DOI: 10.1021/jacs.9b00384
J. Am. Chem. Soc. 2019, 141, 4230−4234

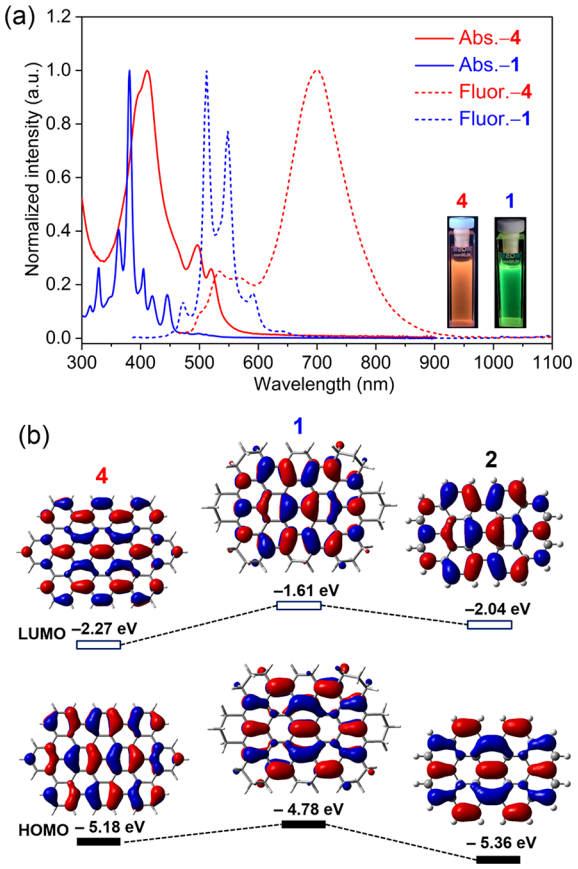

Figure 4. (a) Normalized UV–vis absorption and fluorescence spectra (excited at the absorption maxima) of **1** and **4** in THF solution (2×10^{-5} M) (inset: emission of **1** and **4** under 365 nm wavelength of UV lamp). (b) Frontier molecular orbitals and energy diagrams of **1**, **2** and **4** at the B3LYP/6-311G(d) level. For simplicity of computation, dodecyl chains of **1** and **4** were removed.

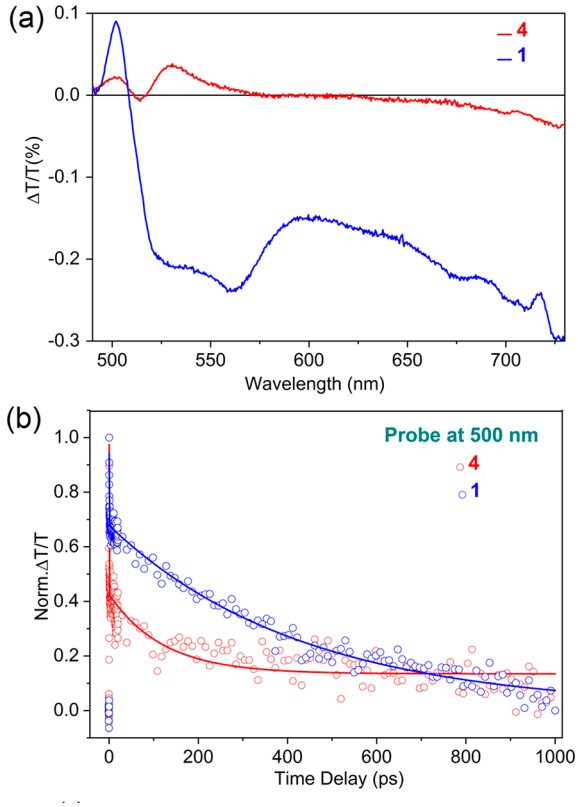

Figure 5. (a) Femtosecond transient absorption spectra of **1** and **4** in THF solution at 1 fs pump–probe delay obtained by exciting at 470 nm and probing with a broadband probe light. (b) Transient dynamics for **1** and **4** at a probe wavelength of 500 nm. The solid blue and red lines represent the biexponential best-fit curves for **1** and **4**, respectively.

is at 555 nm (Figure S9). The weak fluorescence of **4** hindered the determination of its fluorescence quantum yield.

DFT calculations were performed to compare the electronic properties of pristine **4**, peripheral hydrogenated **1** and parent circumbiphenyl **2** (Figure 4b). The HOMO and LUMO energy levels of **4** are calculated to be −5.18 and −2.27 eV, respectively, with a HOMO–LUMO gap of 2.91 eV. Peripheral hydrogenation results in a higher lying HOMO (−4.78 eV) and LUMO energy levels (−1.61 eV) of **1**, with an energy gap of 3.17 eV which is by 0.26 eV greater than that of **4**. These observations are in accordance with the UV–vis experiment, indicating the ability of electronic tuning of PAHs through peripheral hydrogenation. Besides, the DFT-calculated HOMO and LUMO of peralkylated circumbiphenyl **1** reveal the same orbital distribution pattern as that of **2**. In addition, the HOMO–LUMO gap of **1** is smaller than that of **2** (3.32 eV), in line with the red-shifted onset of absorption of **1**.

Ultrafast transient absorption (TA) spectroscopy (see the Supporting Information) discloses the effect of peripheral hydrogenation on the excited state photodynamics of the molecules. Figure 5 presents the TA spectra for **1** and **4** excited at the low-energy absorption edge (470 nm). Interestingly, whereas for **4** we can distinguish two photobleaching (PB) peaks (500 and 530 nm) and a broad photoinduced absorption (PA) from 600 to 750 nm, **1** exhibits a sharp positive band at 500 nm that can be attributed to stimulated emission (SE), as it overlaps with one of the multiple well-resolved fluorescence peaks and cannot be connected to ground state absorption. Note that the other potential SE signals (550 and 600 nm) are overlapped with the strong and broad PA in the midvisible, which is typical for conjugated systems.[21] The reason why **1** displays SE likely lies in its improved solubility brought about by selective peripheral substitution, as we have recently reported that intermolecular interactions in nanographenes lead to the formation of aggregates with charge-transfer character, in which charge generation quenches SE and gain.[22] The TA dynamics (probe at 500 nm, Figure 5b) show a longer lifetime for **1** ($\tau_1 = 0.4 \pm 0.04$ ps; $\tau_2 = 420 \pm 20$ ps) than **4** ($\tau_1 = 0.1 \pm 0.01$ ps ; $\tau_2 = 120 \pm 15$ ps), a result that can also correlate with the poorer solubility of **4** with respect to the hydrogenated molecule. In general, these findings highlight the potential of peralkylated circumbiphenyl **1** for applications in photonics and optoelectronics.

In summary, we have presented hydrogenation as a "π-truncation" strategy leading to the first peralkylated circumbiphneyl **1**. MALDI-TOF MS, 1D and 2D NMR combined with FT-IR and Raman results provided an explicit structure proof of the regiospecific peripheral hydrogenation of nanographene molecule **4**, leading to a peralkylated circumbiphenyl core. Moreover, investigation of **1** by ultrafast transient absorption measurements revealed stimulated emission, which was absent for **4** before the hydrogenation, pointing toward the possible application of such hydrogenated nanographene molecules as optical gain materials, for example to

DOI: 10.1021/jacs.9b00384
J. Am. Chem. Soc. 2019, 141, 4230–4234

develop an organic laser. Considering the directness and efficiency of π-truncation, this strategy could serve as a general approach to other unique aromatic structures not available by π-expansion, providing new candidates for (opto-)electronic devices and supramolecular chemistry.

■ ASSOCIATED CONTENT

Supporting Information

The Supporting Information is available free of charge on the ACS Publications website at DOI: 10.1021/jacs.9b00384.

Materials and methods, synthetic procedure, NMR, Raman, FT-IR spectroscopy and photoluminescence spectroscopy, transient absorption information (PDF)

■ AUTHOR INFORMATION

Corresponding Authors

*narita@mpip-mainz.mpg

*muellen@mpip-mainz.mpg.de

ORCID

Xiao-Ye Wang: 0000-0003-3540-0277

Giuseppe M. Paternò: 0000-0003-2349-566X

Akimitsu Narita: 0000-0002-3625-522X

Klaus Müllen: 0000-0001-6630-8786

Notes

The authors declare no competing financial interest.

■ ACKNOWLEDGMENTS

This work was financially supported by Max Planck Society and the European Union's Horizon 2020 research and innovation programme under Marie-Curie ITN project "iSwitch" (GA No.642196) and under Graphene Flagship (785219 GrapheneCore 2). X. Yao is grateful for the scholarship from China Council Scholarship (CSC).

■ REFERENCES

(1) Fetzer, J. C. *Large (C > = 24) Polycyclic Aromatic Hydrocarbons*; John Wiley & Sons: New York, 2000.

(2) (a) Sun, Z.; Ye, Q.; Chi, C.; Wu, J. Low band gap polycyclic hydrocarbons: from closed-shell near infrared dyes and semiconductors to open-shell radicals. *Chem. Soc. Rev.* **2012**, *41*, 7857−7889. (b) Narita, A.; Wang, X.-Y.; Feng, X.; Müllen, K. New advances in nanographene chemistry. *Chem. Soc. Rev.* **2015**, *44*, 6616−6643. (c) Wang, X.-Y.; Narita, A.; Müllen, K. Precision synthesis versus bulk-scale fabrication of graphenes. *Nat. Rev. Chem.* **2017**, *2*, 0100.

(3) Chen, L.; Hernandez, Y.; Feng, X.; Müllen, K. From Nanographene and Graphene Nanoribbons to Graphene Sheets: Chemical Synthesis. *Angew. Chem., Int. Ed.* **2012**, *51*, 7640−7654.

(4) Feng, X.; Pisula, W.; Müllen, K. J. P. Large polycyclic aromatic hydrocarbons: synthesis and discotic organization. *Pure Appl. Chem.* **2009**, *81*, 2203−2224.

(5) (a) Xiao, S.; Myers, M.; Miao, Q.; Sanaur, S.; Pang, K.; Steigerwald, M. L.; Nuckolls, C. Molecular Wires from Contorted Aromatic Compounds. *Angew. Chem., Int. Ed.* **2005**, *44*, 7390−7394. (b) Chiu, C.-Y.; Kim, B.; Gorodetsky, A. A.; Sattler, W.; Wei, S.; Sattler, A.; Steigerwald, M.; Nuckolls, C. Shape-shifting in contorted dibenzotetrathienocoronenes. *Chem. Sci.* **2011**, *2*, 1480−1486. (c) Daigle, M.; Picard-Lafond, A.; Soligo, E.; Morin, J.-F. Regioselective Synthesis of Nanographenes by Photochemical Cyclodehydrochlorination. *Angew. Chem., Int. Ed.* **2016**, *55*, 2042−2047.

(6) (a) Scott, L. T.; Cheng, P.-C.; Hashemi, M. M.; Bratcher, M. S.; Meyer, D. T.; Warren, H. B. Corannulene. A Three-Step Synthesis1. *J. Am. Chem. Soc.* **1997**, *119*, 10963−10968. (b) Scott, L. T.; Jackson, E. A.; Zhang, Q.; Steinberg, B. D.; Bancu, M.; Li, B. A Short, Rigid, Structurally Pure Carbon Nanotube by Stepwise Chemical Synthesis. *J. Am. Chem. Soc.* **2012**, *134*, 107−110. (c) Scott, L. T.; Boorum, M. M.; McMahon, B. J.; Hagen, S.; Mack, J.; Blank, J.; Wegner, H.; de Meijere, A. A Rational Chemical Synthesis of C_{60}. *Science* **2002**, *295*, 1500.

(7) (a) Clar, E.; Zander, M. 927. Syntheses of coronene and 1:2−7:8-dibenzocoronene. *J. Chem. Soc.* **1957**, 4616−4619. (b) Fort, E. H.; Donovan, P. M.; Scott, L. T. Diels−Alder Reactivity of Polycyclic Aromatic Hydrocarbon Bay Regions: Implications for Metal-Free Growth of Single-Chirality Carbon Nanotubes. *J. Am. Chem. Soc.* **2009**, *131*, 16006−16007. (c) Fort, E. H.; Scott, L. T. Gas-phase Diels−Alder cycloaddition of benzyne to an aromatic hydrocarbon bay region: Groundwork for the selective solvent-free growth of armchair carbon nanotubes. *Tetrahedron Lett.* **2011**, *52*, 2051−2053. (d) Konishi, A.; Hirao, Y.; Matsumoto, K.; Kurata, H.; Kubo, T. Facile Synthesis and Lateral π-Expansion of Bisanthenes. *Chem. Lett.* **2013**, *42*, 592−594. (e) Li, J.; Jiao, C.; Huang, K.-W.; Wu, J. Lateral Extension of π Conjugation along the Bay Regions of Bisanthene through a Diels−Alder Cycloaddition Reaction. *Chem. - Eur. J.* **2011**, *17*, 14672−14680. (f) Schuler, B.; Collazos, S.; Gross, L.; Meyer, G.; Pérez, D.; Guitián, E.; Peña, D. From Perylene to a 22-Ring Aromatic Hydrocarbon in One-Pot. *Angew. Chem., Int. Ed.* **2014**, *53*, 9004−9006.

(8) (a) Zhang, Q.; Kawasumi, K.; Segawa, Y.; Itami, K.; Scott, L. T. Palladium-Catalyzed C−H Activation Taken to the Limit. Flattening an Aromatic Bowl by Total Arylation. *J. Am. Chem. Soc.* **2012**, *134*, 15664−15667. (b) Kawasumi, K.; Zhang, Q.; Segawa, Y.; Scott, L. T.; Itami, K. A grossly warped nanographene and the consequences of multiple odd-membered-ring defects. *Nat. Chem.* **2013**, *5*, 739.

(9) Watson, M. D.; Debije, M. G.; Warman, J. M.; Müllen, K. Peralkylated coronenes via regiospecific hydrogenation of hexa-peri-hexabenzocoronenes. *J. Am. Chem. Soc.* **2004**, *126*, 766−771.

(10) Tashiro, S.; Yamada, M.; Shionoya, M. Iridium-Catalyzed Reductive Carbon−Carbon Bond Cleavage Reaction on a Curved Pyridylcorannulene Skeleton. *Angew. Chem., Int. Ed.* **2015**, *54*, 5351−5354.

(11) Matsuo, Y.; Tahara, K.; Sawamura, M.; Nakamura, E. Creation of hoop-and bowl-shaped benzenoid systems by selective detraction of [60] fullerene conjugation.[10] cyclophenacene and fused corannulene derivatives. *J. Am. Chem. Soc.* **2004**, *126*, 8725−8734.

(12) Clar, E.; Mackay, C. C. Circobiphenyl and the attempted synthesis of 1:14, 3:4, 7:8, 10:11-tetrabenzoperopyrene. *Tetrahedron* **1972**, *28*, 6041−6047.

(13) Xiao, S.; Kang, S. J.; Wu, Y.; Ahn, S.; Kim, J. B.; Loo, Y.-L.; Siegrist, T.; Steigerwald, M. L.; Li, H.; Nuckolls, C. Supersized contorted aromatics. *Chem. Sci.* **2013**, *4*, 2018−2023.

(14) Iyer, V. S.; Yoshimura, K.; Enkelmann, V.; Epsch, R.; Rabe, J. P.; Müllen, K. A Soluble C60 Graphite Segment. *Angew. Chem., Int. Ed.* **1998**, *37*, 2696−2699.

(15) Hudgins, D. M.; Sandford, S. A. Infrared Spectroscopy of Matrix Isolated Polycyclic Aromatic Hydrocarbons. 2. PAHs Containing Five or More Rings. *J. Phys. Chem. A* **1998**, *102*, 344−352.

(16) Wei, J.; Jia, X.; Yu, J.; Shi, X.; Zhang, C.; Chen, Z. Synthesis of 1,4,5,8,9,12-hexabromododecahydrotriphenylene and its application in constructing polycyclic thioaromatics. *Chem. Commun.* **2009**, *31*, 4714−4716.

(17) (a) Wu, J.; Tomović, Ž.; Enkelmann, V.; Müllen, K. From Branched Hydrocarbon Propellers to C3-Symmetric Graphite Disks. *J. Org. Chem.* **2004**, *69*, 5179−5186. (b) Casiraghi, C.; Ferrari, A. C.; Robertson, J. Raman spectroscopy of hydrogenated amorphous carbons. *Phys. Rev. B: Condens. Matter Mater. Phys.* **2005**, *72*, 085401.

(18) Kastler, M.; Pisula, W.; Wasserfallen, D.; Pakula, T.; Müllen, K. Influence of Alkyl Substituents on the Solution- and Surface-Organization of Hexa-peri-hexabenzocoronenes. *J. Am. Chem. Soc.* **2005**, *127*, 4286−4296.

(19) Wasserfallen, D.; Kastler, M.; Pisula, W.; Hofer, W. A.; Fogel, Y.; Wang, Z.; Müllen, K. Suppressing Aggregation in a Large Polycyclic Aromatic Hydrocarbon. *J. Am. Chem. Soc.* **2006**, *128*, 1334−1339.

DOI: 10.1021/jacs.9b00384
J. Am. Chem. Soc. 2019, 141, 4230−4234

(20) Rurack, K. In *Standardization and Quality Assurance in Fluorescence Measurements I: Techniques*; Resch-Genger, U., Ed.; Springer: Berlin-Heidelberg, 2008.
(21) Cabanillas-Gonzalez, J.; Grancini, G.; Lanzani, G. Pump-Probe Spectroscopy in Organic Semiconductors: Monitoring Fundamental Processes of Relevance in Optoelectronics. *Adv. Mater.* **2011**, *23*, 5468−5485.
(22) (a) Paternò, G. M.; Chen, Q.; Wang, X.-Y.; Liu, J.; Motti, S. G.; Petrozza, A.; Feng, X.; Lanzani, G.; Müllen, K.; Narita, A.; Scotognella, F. Synthesis of Dibenzo[hi,st]ovalene and Its Amplified Spontaneous Emission in a Polystyrene Matrix. *Angew. Chem., Int. Ed.* **2017**, *56*, 6753−6757. (b) Paternò, G. M.; Nicoli, L.; Chen, Q.; Müllen, K.; Narita, A.; Lanzani, G.; Scotognella, F. Modulation of the Nonlinear Optical Properties of Dibenzo[hi,st]ovalene by Peripheral Substituents. *J. Phys. Chem. C* **2018**, *122*, 25007−25013.

DOI: 10.1021/jacs.9b00384
J. Am. Chem. Soc. 2019, 141, 4230−4234